

# Detection and Recognition of License Plate Characters with Different Appearances

Shen-Zheng Wang and Hsi-Jian Lee

Department of Science and Information Engineering, National Chiao-Tung University  
1001 Ta Hsueh Road, Hsinchu, Taiwan 300, R.O.C.  
e-mail: sgwang@csie.nctu.edu.tw, hjee@csie.nctu.edu.tw

**Abstract**—This paper proposes an approach to developing an automatic license plate recognition system. Car images are taken from various positions outdoors. Because of the variations of angles from the camera to the car, license plates have various locations and rotation angles in an image. In the license plate detection phase, the magnitude of the vertical gradients is used to detect candidate license plate regions. These candidate regions are then evaluated based on three geometrical features: the ratio of width and height, the size and the orientation. The last feature is defined by the major axis. In the character recognition phase, we must detect character features that are non-sensitive to the rotation variations. The various rotated character images of a specific character can be normalized to the same orientation based on the major axis of the character image. The crossing counts and peripheral background area of an input character image are selected as the features for rotation-free character recognition. Experimental results show that the license plates detection method can correctly extract all license plates from 102 car images taken outdoors and the rotation-free character recognition method can achieve an accuracy rate of 98.6%.

**Index Terms**—Character recognition, license plate detection, license plate recognition, image orientation detection, rotation-free character recognition.

## I. INTRODUCTION

THE development of Intelligent Transportation System (ITS) has grown rapidly over the last ten years. With the progress of the computer vision technologies, data such as license plate numbers can be obtained automatically. These data can be used in follow-up analyses and monitors. The following shows the input images from LPR outdoors. Figure 1 shows the images of the outdoor cars captured from digital sensors with different relative locations from the camera to the car and different appearances of the license plate may appear in the images. Figure 2 shows two different appearances of the license plates. Previous researches [1]-[10] on optical character recognition (OCR) in license plate recognition systems generally assumed that the text lies in a plane whose angles were roughly

perpendicular to the optical axis of the sensor and did not consider the rotation situation. Under the assumption, various approaches to recognizing characters were studied, but those approaches failed to handle the rotation distortion as shown in Figs. 1 and 2. The range of the sensor position (pan/tilt) reported in previous studies is less than  $20^\circ$ , which does not work well in the license plate recognition system used outdoors, because the license plates appearing in captured images usually have more than  $20^\circ$  relative location (pan/tilt).

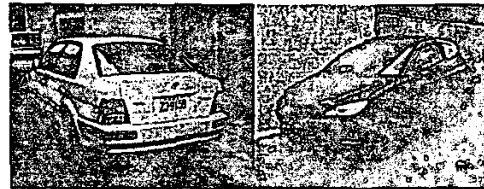


Fig. 1: Images of the cars with different relative locations.



Fig. 2: Two different appearances of the license plates in Fig. 1.

In order to extend the application of license plate recognition into various fields, it is necessary to develop an OCR algorithm to handle more deformable images. In general, LPR system includes two main modules: (1) license plate detection and (2) character segmentation and recognition. The license plate detection phase proposed in this paper can detect all license plates of the car images without constraints in relative locations and directions from the camera to the car. The character recognition phase presented in this paper can recognize characters with various rotation angles since the characters are normalized with respect to the major axis. The remaining parts of this paper are organized as follows. Section II studies the motivation and modules of the orientation normalization. Section III presents the procedure of license plates detection. Section IV describes the rotation-free license plate recognition module and Section V shows experimental results. The final part of the paper includes some concluding remarks.

## II. ORIENTATION NORMALIZATION

This paper aims to detect the license plates of the car image with various locations and to recognize the rotation-free characters in the license plates. It is useful to derive the major axis which shows the orientation of the image to detect and recognize license plates. In the license plate detection phase, the major axis is measured in possible license plate region to evaluate the possibility to be a license plate region. Figure 3 shows the major axis on each image of the character "R" in five different rotation angles, where the dash lines represent the major axis of the character image. In the character recognition phase, the character images are rotated to a normalized coordinate system with respect to the major axis.

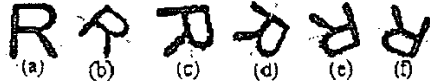


Fig. 3: The images of character "R" in different orientations. The dash lines represent the major axis.

### A. Orientation Detection

In the binary image, we first define that the mass is the black pixels whose gray level is 1. The moment of mass of the binary image is the distribution of the mass throughout the binary image. Horn [11] mentioned that the first moment of mass which is defined as mass times distance could be used to derive the center location of the mass and the second moment of the mass could be measured the distribution of mass relative to axes through the center of the mass. And the orientation,  $\theta$ , of the mass is derived from the least second moment of the mass. Then, the major axis of the mass can be achieved from the orientation  $\theta$  and the center. The steps to derive the orientation from the binary image are described in the following.

The first moment of mass in the binary image is defined as

$$C = (x_c, y_c) = \left( \iint xg(x, y)dx dy, \iint yg(x, y)dx dy \right) \quad (1)$$

where  $g(x, y)$  is the black point  $(x, y)$  which gray level is 1 in the binary image.

The second moment of mass in the binary image is equal to mass times square of the distance from the black point in the binary image to a line  $L$  as shown below:

$$S = \iint r^2 g(x, y) dx dy \quad (2)$$

where  $r$  is the perpendicular distance from the black point  $(x, y)$  to a line  $L$ . In Fig. 4, for a particular line  $L$  in the binary image, two parameters are defined: the distance  $t$  from the origin to the closest point on the line, and the angle  $\theta$  between the x-axis and the line, which is measured counterclockwise. The equation of the line  $L$  is presented as follows.

$$x \sin \theta - y \cos \theta + t = 0 \quad (3)$$

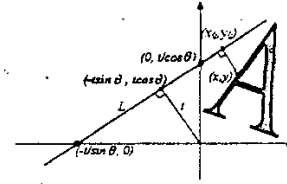


Fig. 4: The coordinate diagram.

Suppose that the distance from the point  $(x_0, y_0)$  located on the line  $L$  to the point  $(-t \sin \theta, t \cos \theta)$  is  $\gamma$ .

$$\begin{aligned} x_0 &= -t \sin \theta + \gamma \cos \theta \text{ and} \\ y_0 &= t \cos \theta + \gamma \sin \theta. \end{aligned} \quad (4)$$

Given an arbitrary black point  $(x, y)$  in the binary image, the shortest distance  $r$  between  $(x, y)$  and the line  $L$  is defined as

$$\begin{aligned} r^2 &= (x - x_0)^2 + (y - y_0)^2 \\ &= t^2 + 2t(x \sin \theta - y \cos \theta) - 2\gamma(x \cos \theta + y \sin \theta) + \gamma^2 + (x^2 + y^2) \end{aligned} \quad (5)$$

By differentiating with respect to  $\gamma$  and substituting back into the equation (2), the second moment of mass can be derived as

$$S = \iint (x \sin \theta - y \cos \theta + t)^2 g(x, y) dx dy \quad (6)$$

Without losing the generality, we change the coordinate to  $x' = x - x_c$  and  $y' = y - y_c$ . By substituting the equation (1) into the equation (6) and totally differentiating with respect to  $t$ , we obtain

$$\begin{aligned} S &= \iint \left( (x')^2 \sin^2 \theta + 2(x'y') \sin \theta \cos \theta + (y')^2 \cos^2 \theta \right) g(x, y) dx' dy' \\ &= \iint \left( \frac{1}{2} ((x')^2 (1 - \cos 2\theta) + 2(x'y') \sin 2\theta + (y')^2 (\cos 2\theta - 1)) \right) g(x, y) dx' dy' \\ &= \frac{1}{2} \iint \left( ((x')^2 + (y')^2) - ((x')^2 - (y')^2) \cos 2\theta - 2(x'y') \sin 2\theta \right) g(x, y) dx' dy' \end{aligned} \quad (7)$$

Total differentiating  $S$  with respect to  $\theta$  and we can obtain

$$\theta = \frac{1}{2} \arctan \left( \frac{\iint 2(x'y') dx' dy'}{\iint ((x')^2 - (y')^2) dx' dy'} \right) \quad (8)$$

The major axis in the binary image is defined as the line which slope is  $\theta$  and the major axis crosses the center.

## III. LICENSE PLATES DETECTION

Due to the similar colors of the license plate background and that of the car body, it is difficult to detect the boundary of the license plate from the input car images in outdoors. Because the color of characters is different from that of the license plate background, the gradients of the original image are adopted to detect candidate license plate regions. Figure 5 shows the

processing flow of license plates detection.

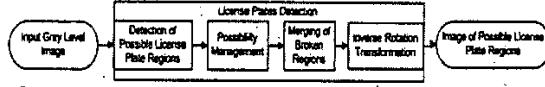


Fig. 5: Processing flow of license plate detection.

#### A. Detection of Possible License Plate Regions

At the first step of the license plate detection phase, the possible license plate regions are detected from the gradients of the input car images. The gradients are derived by multiplying with a mask value for each pixel and its neighboring pixels. The Sobel operator [9][12] uses two masks to find vertical and horizontal gradients. Since the license plates are located on the bumper, in the car images, the license plate region is usually connected with horizontal lines. Figure 6(a) shows the license plate image. Figure 6(b) displays the Sobel gradients of Fig. 6(a). Figure 6(c) and Fig. 6(d) exhibit the vertical and horizontal gradients of Fig. 6(a). It is hard to separate the license plate region from the others in the horizontal gradients image with. But it is easy to detect the license plate region from the vertical gradients image because the magnitude of vertical gradients is strong in the characters of the license plate image while weak in the vertical lines. In the vertical gradients image, the license plate region is the area with large local variance. The local variances of the vertical gradients image are measured by the equation (9).



Fig. 6: (a) The license plate image; (b) (c)(d) The Sobel gradients, the vertical gradients and the horizontal gradients of Fig. 6(a) respectively.

$$\begin{aligned}
 LocalVar(i, j) &= \sum_{i,j \in W} \frac{g^2(i, j)}{N_s} - \left( \frac{\sum_{i,j \in W} g(i, j)}{N_s} \right)^2 \\
 &= \sum_{i,j \in W} \frac{1}{N_s} \left( \begin{bmatrix} f(i-1, j-1) & f(i, j-1) & f(i+1, j-1) \\ f(i-1, j) & f(i, j) & f(i+1, j) \\ f(i-1, j+1) & f(i, j+1) & f(i+1, j+1) \end{bmatrix} \cdot \begin{bmatrix} -101 \\ -202 \\ -101 \end{bmatrix} \right)^2 \\
 &\quad - \frac{1}{(N_s)^2} \left( \sum_{i,j \in W} \begin{bmatrix} f(i-1, j-1) & f(i, j-1) & f(i+1, j-1) \\ f(i-1, j) & f(i, j) & f(i+1, j) \\ f(i-1, j+1) & f(i, j+1) & f(i+1, j+1) \end{bmatrix} \cdot \begin{bmatrix} -101 \\ -202 \\ -101 \end{bmatrix} \right)^2
 \end{aligned} \quad (9)$$

where  $W$  is the local window mask,  $g(i, j)$  is the magnitude of the gradients image,  $N_s$  is the size of  $W$ ,  $\bullet$  is the inner product operator and  $f(i, j)$  denotes the gray level of the original image. In order to cover the characters in the license plate of the input car images, the size of the local window mask,  $W$ , is set as  $11 \times 7$ . There may be some noise in the images of possible license plates such as holes and single dots. An opening operation of morphological analysis, in which the dilation operation is performed after an erosion operation, is applied in order to reduce the undesired effect of noise and to separate the regions that were slightly connected.

#### B. Possibility Measurement

To detect the most possible license plate regions from the candidate plate regions, the geometrical properties of the license plate are introduced to measure the possibility value. The following defines the geometrical features: 1) *Area*: If the candidate region is large, it is more likely being a license plate. A higher possibility value represents a more possible license plate region. The possibility of the area is defined as  $N_s / \sum N_s$  where

$N_s$  is the number of boundary rectangle of the possible license plate region,  $s$ . 2) *Orientation*: As described in Section II, the orientation of each possible license plate region can be measured. A license plate usually appears as a horizontal rectangle. The smaller the orientation of the possible license plate region is, the higher the possibility value is. The possibility of the orientation is given by  $(90 - \theta_s) / 90$  where  $\theta_s$  is the orientation of the possible license plate region,  $s$ . 3) *Density*: The ratio between the black regions and the area of the bounding rectangle is defined as the density of the license plate region. The license plate is always a rectangle. A higher density value means that the region is more likely to be a rectangle and to be viewed as a license plate region. The possibility of the density is defined as  $B_s / N_s$  where  $B_s$  is the number of the possible license plate region,  $s$ . For each possible license plate region,  $s$ , the possibility value,  $p(s)$ , is defined as the weighted sum of the above three features, as shown below.

$$\begin{aligned}
 p(s) &= p(\text{area}, \text{orientation}, \text{density}) \\
 &= \omega_1 \frac{N_s}{\sum N_s} + \omega_2 \frac{90 - \theta_s}{90} + \omega_3 \frac{B_s}{N_s} \quad (10)
 \end{aligned}$$

where  $\omega_i$  is the weighting coefficient. We need to select proper  $\omega_i$  that can keep a high detection rate. These values are determined according to experimental results. In this paper,  $\omega_1 = 0.2$ ,  $\omega_2 = 0.3$  and  $\omega_3 = 0.5$  are adopted.

#### C. Merging of Broken Regions

After the detection of all candidate license plate regions, a license plate is probably separated into several adjacent regions. Assume that  $s1$  and  $s2$  are two possible license plate regions and  $s$  is the merged region of  $s1$  and  $s2$ . Regions  $s1$  and  $s2$  are merged when the following two rules are satisfied. 1) The distance between  $s1$  and  $s2$  is smaller than a threshold value. 2) The possibility value of the merged regions is larger than both of  $s1$  and  $s2$ . The merging operation is repeatedly performed until no regions could be merged. Then, the region with the largest possibility value is viewed as the license plate region.

### IV. ROTATION-FREE LICENSE PLATE RECOGNITION

In the rotation-free license plate recognition phase, there are five main steps includes as shown in Fig. 7. To extract the

characters in the license plate images, we binarized the license plate images. The robust dynamic threshold method, Otsu, proposed in [15] is applied. The de-noise process is then applied to eliminate small regions and the boundary. Figure 8(a) shows the license plate images extracted from Fig. 8(a) and Fig. 8(b) displays the binarized and de-noised result.

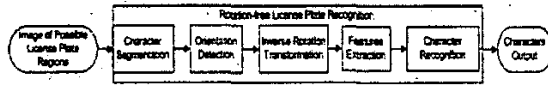


Fig. 7: Processing flow of the rotation-free character recognition module.

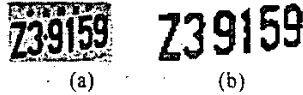


Fig. 8: (a) The license plate image; (b) The binarized and de-noised result.

Second, the characters in the license plate images are segmented into single ones. For each character image, the major axis and inverse rotation transformation are performed to normalize the character image. For each normalized character image, we can extract similar features even if the original character image has various rotations.

#### A. Character Segmentation

Given a binarized license plate image, the orientation is obtained. Then, the connected-component based method is used to segment the image into single characters. The characters of the connected-components are confirmed by two properties of the license plate: (1) The digits on the license plate are fixed on car license plates; (2) The characters lie in horizontal orientation. When the fixed numbers of character components in the license plate image are not obtained or the major axis of the binarized license plate image does not cross through all the character components, the license plate image is rejected. Due to the possible various rotation angles of the characters in the input image, the major axis of each single character is measured and the inverse rotation transformation is performed to normalize the character image.

#### B. Features Extraction

Before character recognition, we must extract significant features that tolerate variations among samples of the same character and differentiate variations in different characters. In order to implement the robust OCR system, the input character image is rotated to a normalized coordinate system at the preceding process. But when the tilt/pan angles from the camera to the car are various, the flat/thin character images may be obtained as shown in Fig. 9(b) and Fig. 9(c).

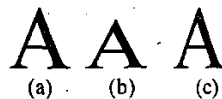


Fig. 9: Three different types of the character "A".

Tu *et al.* [14] suggested using the features called contour-crossing counts to collect the number of boundary

pixels of characters. To tolerate variations among the images of the same characters, the input character image is divided into 64 sub-images by the orientation described in Section II. And the crossing-count features that are the number of strokes are extracted from the sub-images. The extraction method of non-uniform crossing-count features is described below. And another feature, peripheral background area (PBA) [13], is used to calculate the outer area from the character boundary to the image boundary. We have selected the two statistical features to implement our OCR engine.

1) *Extraction of Crossing-count Features (CCFs)*: In order to accommodate tilt/pan variations, the character image is first segmented into quarter by the major axis and the line which is perpendicular to the major axis. Each sub-image of the quarter is then segmented non-uniformly into 4 strips in both the horizontal and vertical directions. These strips have the same numbers of black pixels as shown in Fig. 13. And in order to speed up the extraction, four scan lines are selected to extract features in each strip. In Fig. 10, the  $CC_k$  which is the number of strokes intersecting each scan line  $k$  which is shown as the dash line is counted where  $k = 1$  to 4. The feature dimension of CCFs is  $64 (= 16 \times 4)$ . And the feature vector is processed to the next character recognition phase. The feature value  $f_i$  in strip  $i$  is defined as follows:

$$f_i = \sum_{k=1}^4 CC_{ik}, i = 1, 2, \dots, 16 \dots \dots \dots (11)$$

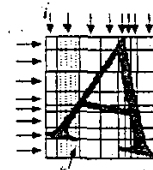


Fig. 10: The crossing-count features.

2) *Extraction of Peripheral Background Area Features (PBAFs)*: Peripheral background area feature is the length of line segments which are from the boundary of the image to the character contour. First the input character image is segmented into 16 strips in both the horizontal and vertical directions by the method described at above processing. In each strip, two values of length from both of the image boundary to the character contour divided by the length of the strip are measured. The feature dimension of PBA is  $32 (= 16 \times 2)$ .

#### C. Character Recognition

For each of the two features, let the feature vector  $x$  derived from an input character image and let the vector  $\mu_j$  be the mean vector of the reference character  $j$ . Also let the vector  $\sigma_j$  be the standard deviation accompanying each feature of character  $j$ . Tseng *et al.* [13] presented the following discriminant function for character recognition:

$$d(x, \mu_j) = \sum_{i=1}^K \frac{(x_i - \mu_{ji})^2}{\sigma_{ji}^2} + c \times \log(\sigma_{ji}^2) \quad (12)$$

where  $c$  is a constant obtained from the training data. The combined discriminant function is defined as

$$Cb = w_1 d(CCFs, \mu_j) + w_2 d(PBAFs, \mu_j) \quad (13)$$

where  $w_1$  and  $w_2$  are the coefficients which are determined according to experimental results. In this paper,  $w_1$  and  $w_2$  are set as 0.7 and 0.3 respectively. We evaluate the combined discriminant function between the input character and each reference character, and then choose the smallest one among them as the recognized character.

## V. EXPERIMENTAL RESULTS

The system proposed in this paper has been applied to 102 images with 104 license plates, involving vehicles at different pan/tilt angles. We implemented the proposed system on a Pentium II 300MHz PC with C++ language under Windows environment and used Nikon 5700 digital camera as an input device. For the license plate detection method, Fig. 11 shows the original car images, the possible license plate regions and the result image of license plate detection. There are 108 totally license plate images extracted from the test images. The false license plate can be rejected in the character segmentation phase described in Section IV.A. But when the over detected license plate region is detected such as shown in Fig. 12, it is also rejected in the character segmentation phase. In Fig. 12, the size of characters on the spare tire is similar to the size of characters on license plate. In this paper, the license plate of such images can be detected but can not be recognized. The accuracy rates of recognition are listed in Table 1 and Table 2. There were 624 characters extracted from the license plate images.

## VI. CONCLUSION

In this paper, we have proposed an automatic license plate detection and rotation-free character recognition system. In conventional license plate detection and recognition methods, it is difficult to determine the license plate with large pan and tilt angles and is hard to recognize the rotation-free characters. The proposed methods use major axis information which is non-sensitive to rotation variance to detect the license plate and normalize the character to the same orientation. The major axis is determined by the orientation which is the second moment of the mass and center which is the first moment of the mass in the binary image. Then, the input images can be taken from large pan and tilt angles relative to the car in outdoors. Experiments carried out on some samples of outdoors car images show the feasibility of using the proposed methods to detect and recognize the license plate. The system proposed can be applied in general security systems and car violation prevention systems.

## ACKNOWLEDGMENT

This work was supported by the Nation Science Council, under grant NSC-91-2213-E-009-105.

## REFERENCES

- [1] P. Comelli, P. Ferragina, M. N. Granieri, and F. Stabile, "Optical recognition of motor vehicle license plates," *IEEE Trans. on Vehicular Technology*, vol. 44, no. 4, pp. 790-799, 1995.
- [2] H. J. Kim, D. W. Kim, S. K. Kim, and J. K. Lee, "Automatic recognition of a car license plate using color image processing," *Journal of Engineering Design and Automation*, Vol. 3, No. 1, 1997.
- [3] S. K. Kim, D. W. Kim, and H. J. Kim, "Recognition of vehicle license plate using a genetic algorithm based segmentation," in *Proc. of IEEE International Conference on Image Processing*, Lausanne Switzerland, Sep 16-19 1996, pp. 661-664.
- [4] C. Coetzee, C. P. Botha and D. Weber, "PC based number plate recognition system," in *Proc. IEEE International symposium on Industrial Electronics*, Pretoria, South Africa, vol. 2, July 1998, pp. 604-610.
- [5] Y.-T. Cui and Q. Huang, "Character extraction of license plates from video," in *Proc. Computer Society Conference on Computer Vision and Pattern Recognition*, St. Puerto Rico, June 17-19, 1997, pp. 502-507.
- [6] H. Kurosaki, M. Yagi and H. Yokosuka, "Vehicle license number recognition system for measuring travel time," *Journal of Robot. Mechatron*, vol. 5, no. 2, pp. 192-197, 1993.
- [7] G. Auty, et al., "An image acquisition system for traffic monitoring applications," in *Proc. SPIE*, vol. 2416, 1995, pp. 119-133.
- [8] S. H. Park, K. L. Kim, K. Jung and H. J. Kim, "Locating car license plates using neural networks," *IEEE Electronics Letters*, Vol. 35, No. 17, pp. 1475-1477, Aug. 1999.
- [9] K. M. Kim, B. J. Lee, K. Lyoo and G. T. Park, "The automatic recognition of the plate of vehicle using correlation coefficient and Hough transform," *Journal of Control Automation and System Engineering*, 3(5):511-519, 1997.
- [10] D. U. Cho and Y. H. Cho, "Implementation of preprocessing independent of environment and recognition of car number plate using histogram and template matching," *Journal of the Korean Institute of Communication Sciences*, 23(1):94-199, 1998.
- [11] B. K. P. Horn, *Robot Vision*, MIT Press, London, 1986.
- [12] R. C. Gonzalez and R. E. Woods, *Digital Image Processing*, 2<sup>nd</sup> Ed., Prentice Hall, N. J., 2002.
- [13] Y. H. Tseng, C. C. Kuo and H. J. Lee, "Speeding-up Chinese character recognition and its application on automatic document reading," *Pattern Recognition*, vol. 31, no. 11, pp. 1589-1600, 1998.
- [14] L. Tu, et al., "Recognition of handprinted Chinese characters by feature matching," in *Int. Conf. on Computer Processing of Chinese and Oriental Languages*, 1991 pp. 154-157.
- [15] N. Otsu, "A threshold selection method from gray-level histograms," *IEEE Trans. on System Man and Cybernetics*, vol. 9, no. 1, Jan 1979, pp. 62-66.

TABLE I  
RECOGNITION RESULTS OF ROTATION-FREE CHARACTER RECOGNITION

No. of Car Images / License Plates	No. of Extracted License Plate	No. of Rejected License Plate
102/104	108	10

TABLE II  
RECOGNITION RESULTS OF ROTATION-FREE CHARACTER RECOGNITION

Extracted License Plate Characters	Successfully Recognized Characters	Accuracy
588	580	98.6%

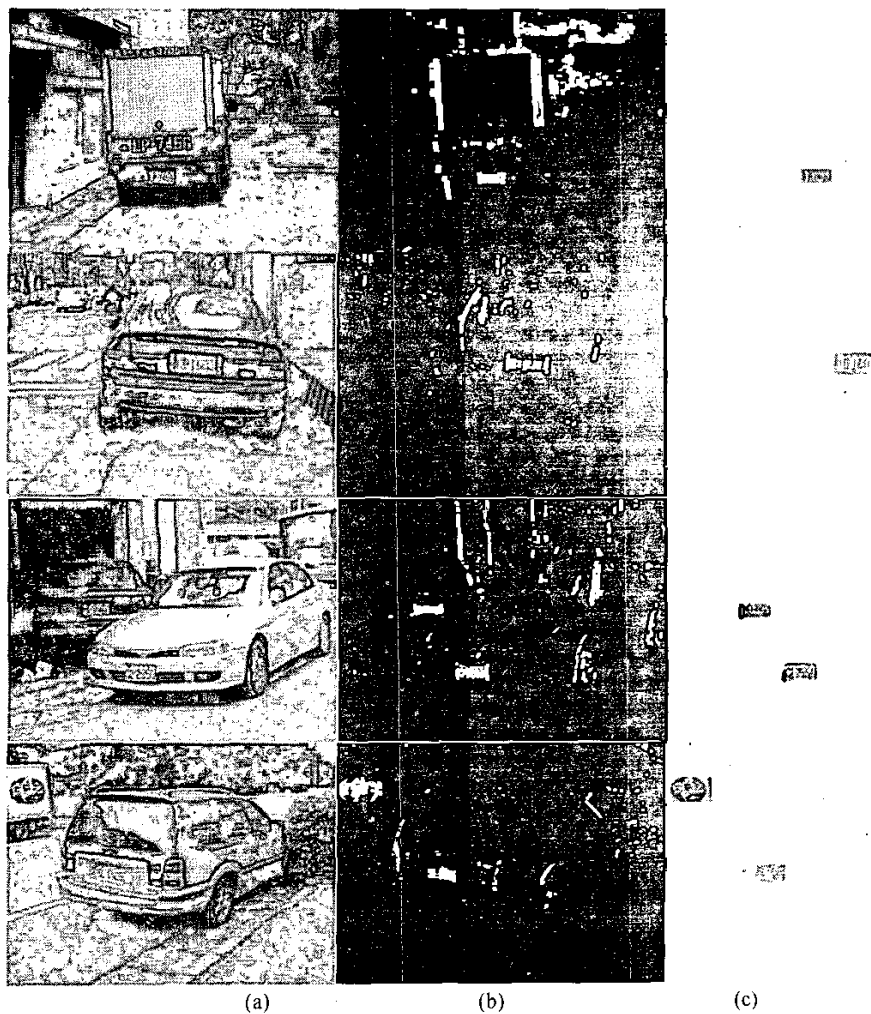


Fig. 11: (a) The car images with license plates; (b) The possible license plate regions; (c) The license plate detection results.

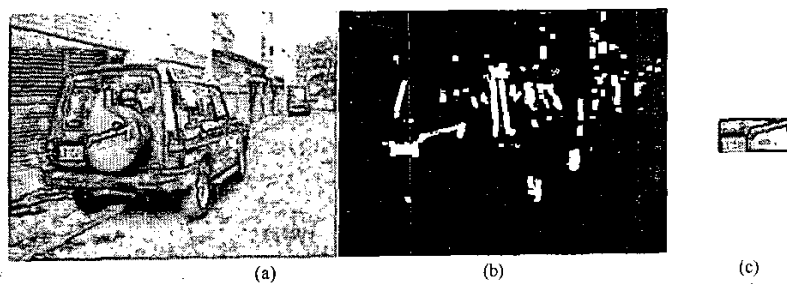


Fig. 12: (a) The car image with a license plate; (b) The possible license plate regions; (c) The license plate detection result.